Hindawi
Geofluids
Volume 2022, Article ID 1356735, 11 pages
https://doi.org/10.1155/2022/1356735

Research Article

Mechanical Properties of Different Lithological Rocks: A Case Study of the Coal Measure Strata in the Eastern Margin of Ordos Basin, China

Xiong Jian,[1] **Wu Jianjun**,[2] **Liu Junjie**,[1] **Li Bing**,[2] **Liu Xiangjun**,[1] **and Liang Lixi**[1]

[1]*State Key Lab of Oil & Gas Reservoir Geology and Exploitation, Southwest Petroleum University, Chengdu 610500, China*
[2]*PetroChina Coalbed Methane Company Limited, Beijing 100028, China*

Correspondence should be addressed to Xiong Jian; 361184163@qq.com

Received 6 January 2022; Revised 9 February 2022; Accepted 28 June 2022; Published 20 July 2022

Academic Editor: Guozhong Hu

In this paper, the mechanical behaviors of different lithological rocks of coal measure strata from Shanxi Formation in the eastern margin of the Ordos Basin, China, were investigated through uniaxial compression tests, and the deformation characteristics and failure modes of different lithological rocks were investigated. On this basis, the energy evolution of different lithology rocks was also discussed. The results show that there are obvious differences in the mechanical properties of different lithology rocks in coal measure strata, resulting in different wellbore instability prevention measures and fracturing measures in different lithology strata. Under the uniaxial compression condition, the peak strain of different lithological rocks is obviously different, and the denaturation characteristics are also obviously different, and the failure modes of rocks are mainly the tensile fracture mode, suggesting that the rock samples have strong brittle characteristics. With the increase of the strain, the total energy of different lithological rocks of the coal measure strata increases, and the elastic energy first increases and then decreases rapidly, whereas the dissipated energy first increases slowly and then increases rapidly. Each energy at the peak point is different, and the average total energy of shale, silty shale, siltstone, fine sandstone, and coal is 0.022 J/cm^3, 0.045 J/cm^3, 0.052 J/cm^3, 0.042 J/cm^3, and 0.003 J/cm^3, respectively, indicating that there are obvious differences in the energy evolution laws of the different lithological rocks.

1. Introduction

In recent years, China's energy demand has increased rapidly, and its dependence on crude oil and natural gas has exceeded 70% and 40%, respectively, which has seriously affected China's energy security. For China, it is necessary to further strengthen the exploration and development of domestic oil and gas [1]. Coal measure natural gas generally refers to all kinds of natural gas existing in coal measure strata, including coalbed methane dominated by adsorption phase, tight sandstone gas dominated by free phase, and shale gas with coexistence of adsorption phase and free phase. Vertically, the coal measure strata are multilayer superimposed reservoir groups of coalbed methane, shale gas, and tight sandstone gas [2, 3]. In the process of single reservoir development, the natural gas production is lower than expected and the resources cannot be fully utilized. The combined exploitation of natural gas in different lithological reservoirs can effectively improve the development and utilization efficiency of coal measure gas resources [4–6]. In the process of combined mining, multilayer hydraulic fracturing is implemented to improve the comprehensive development effect of coal measure natural gas [7–9]. Reservoir geomechanics parameters generally involve rock mechanics, pore pressure, in-situ stress, and other parameters, among which rock mechanics parameters are the basis of reservoir geomechanics research [10]. At the same time, rocks are composed of different mineral types and formed under complex geological processes [11]. In the process of rock deformation and failure, the accumulation and release of energy are the essence of rock failure [12, 13]. The deformation and failure process of rock mass

is an energy-driven instability phenomenon, which is closely related to the energy conversion in this process [14]. The energy evolution law of body deformation and failure has important application in hydraulic fracturing of horizontal and vertical wells. This shows that it is very necessary to investigate the laws of rock mechanics and energy evolution lithological rocks of the coal measure strata.

At present, scholars have carried out a large number of experimental studies on the mechanical properties of rock. YW. Li et al. [15], Eleni et al. [16], Piyush et al. [17], Li et al. [18], and Bagde et al. [19] conducted a lot of research on the mechanical properties of different lithology rocks such as shale, sandstone, and carbonate, and discussed the effects of confining pressure on rock mechanical properties. The fundamental reason for the differences in mechanical properties of different lithological rocks is revealed. At the same time, predecessors have also carried out a large number of experimental studies on the laws of rock energy evolution. Selahattin et al. [20] analyzed the strain fracture tendency of granite based on the post-peak energy evolution of granite. Chen et al. [21] compared and analyzed the energy evolution mechanism of Jurassic and Cretaceous argillaceous sandstone in the Northern Xinjiang, China. Jiang et al. [22] studied the effects of different water content and confining pressure on the energy evolution of mudstone based on the uniaxial and triaxial compression experiments. Yang et al. [23] studied the influences of loading mode on rock deformation characteristics and energy evolution characteristics. The above research results provide an important reference for investigating the energy evolution characteristics of different lithological rocks such as coal, marble, mudstone, and sandstone. In the eastern margin of the Ordos Basin, the vertical superposition relationship of different lithology such as coal, sandstone, shale, and limestone is complex, the horizontal lithology changes frequently [24–26], and there are obvious differences between oil and gas reservoirs with different lithology.

Therefore, taking the rocks of the coal measure strata from Shanxi formation in the eastern margin of Ordos Basin as the research object, the mechanical behaviors of different lithological rocks through uniaxial compression tests are investigated, and the compressive characteristics, deformation characteristics, and failure modes of different lithological rocks are studied, so as to reveal the mechanical properties of different lithological rocks in the coal measures. On this basis, the energy evolution laws of different lithological rocks are discussed.

2. Samples and Methods

2.1. Geological Settings. The eastern margin of Ordos Basin crosses Shanxi and Shaanxi provinces, borders Lishi fault in the East, the Yellow River and Hancheng-Heyang-Tongchuan area in the west, in a narrow and long arc belt, about 450 km long from North to South and 26~100 km wide from East to West, with a total area of $4.5 \times 10^4\,km^2$ [24–26]. Topographically, it is a large West trending gentle slope structure with high North, low South, high East, and low West [24–26]. The coal measure strata in the study area are the Benxi Formation, Taiyuan Formation, and Shanxi Formation from bottom to top. The sedimentary system dominated by barrier coast lagoon system is developed in the Benxi Formation and Taiyuan Formation, while the coastal shallow sea lagoon tidal delta sedimentary system is developed in Shanxi Formation, which is a typical marine land transitional facies sedimentary environment [25–28]. The coal measure strata of these different sedimentary systems have different reservoir combinations of "coalbed methane-tight sandstone gas-shale gas." The sedimentary systems of different layer groups differ greatly, resulting in more obvious differences in the lithology developed in different layer groups, and the reservoir types of the Shanxi Formation with transitional phase sedimentary characteristics are mostly the multilayered superposition of coal-bed methane and tight gas reservoirs, interspersed with shale gas reservoirs.

2.2. Experimental Method. In order to investigate the differences in mechanical properties and energy evolution lows of different lithological rocks of the coal measure strata from the Shanxi Formation in the eastern margin of Ordos Basin, such as coal rocks, siltstones, and fine sandstones, shale and siltstone shale were selected as sample preparation objects. Two rock samples were drilled for each lithology and subjected to uniaxial compression test. According to the Chinese Standards GB/T 23561.7-2009 and GB/T 23561.9-2009, samples for uniaxial compression tests are cylinders with a diameter of 25 mm and length of 50 mm. The nonparallelism of the cylinder end face shall not exceed 0.05 mm, and the end face also shall be perpendicular to the axis, with a maximum deviation less than 0.25°. Uniaxial compression tests were carried out on rtr-1000 high-temperature and high-pressure rock triaxial mechanical test system. The maximum axial loading capacity of the test system is 1000KN and the maximum confining pressure loading capacity is 140 MPa. The RTR-1000 rock triaxial testing system can be shown in Figure 1. During the tests, the axial deformation and radial deformation were determined by the linear variable differential transducers (LVDT) and circumferential sensor, respectively.

According to the test results, the differences of uniaxial compressive strength, elastic modulus, and Poisson's ratio of rocks with different lithology were calculated. On this basis, the energy evolution laws of different lithological rocks were discussed. During the uniaxial compression test, the displacement control mode was used during the experiment, and the strain loading rate of 0.2 mm/min was used for continuous loading of axial load until the rock samples were damaged in order to obtain the stress-strain curves. On the basis, the UCS, E_s, and ν_s can be calculated as follows:

$$UCS = P/A, \tag{1}$$

$$E_s = \Delta\sigma/\Delta\varepsilon, \tag{2}$$

$$\nu_s = |\varepsilon_r/\varepsilon_a|, \tag{3}$$

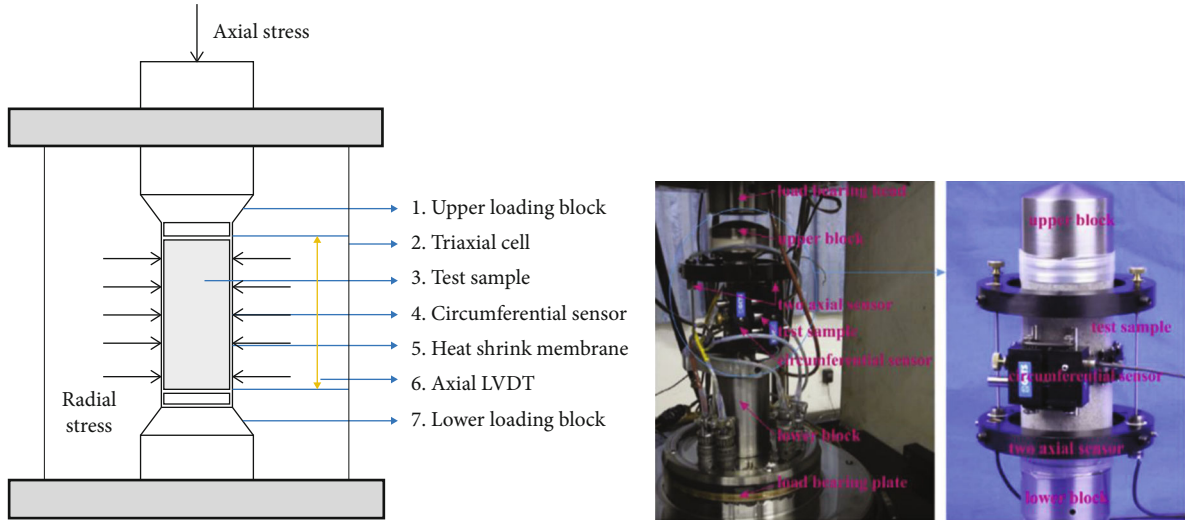

Figure 1: The experimental setup. (a) Schematic diagram of the sample in the triaxial cell; (b) RTR-1000 rock triaxial testing system (revised from the literature [29]).

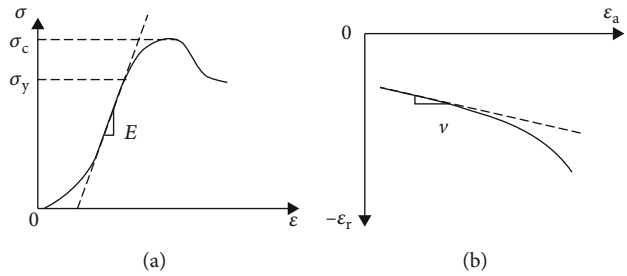

Figure 2: The calculation of Young's modulus (a) and Poisson's ratio (b) based on the elastic deformation stage of the stress–strain curve.

where P is the failure load, kN; A is the cross-sectional area of the sample, m; $\triangle\sigma$ is axial stress of the elastic deformation stage of the stress–strain curve, MPa; $\triangle\varepsilon$ is axial strain of the elastic deformation stage of the stress–strain curve, %; ε_r is radial strain of the elastic deformation stage of the stress–strain curve, %; ε_a is axial strain of the elastic deformation stage of the stress–strain curve, %. The calculation of the E_s and ν_s parameters based on the elastic deformation stage of the stress–strain curve can be seen in Figure 2.

3. Results

3.1. Failure Mode. The failure mode of rock samples with different lithology under uniaxial compression test is shown in Figure 3. By observing Figure 3, it is found that the failure modes of different lithological rock samples are mainly splitting failure mode, which is multiple through cracks approximately parallel to the axis of the rock sample are formed on the rock samples, may be accompanied by secondary fractures that do not penetrate the rock samples. It should be noted that the local shear failure occurs in different lithological rock samples, forming multiple low angle shear fractures. At the same time, we can also see from the figure that in addition to the single or two through fractures formed by fine sandstone, after the failure and instability of shale, silty shale, siltstone, and other rock samples, there are also multiple through fractures approximately parallel to the axis of the rock sample, and with the emergence of multiple secondary fractures, a more complex fracture network is formed. From this point of view, it shows that these rock samples have obvious brittle characteristics.

3.2. Mechanical Properties. Based on the uniaxial compression test, the uniaxial compressive strength, elastic modulus, and Poisson's ratio of different lithological rocks are obtained. The statistical results are shown in Figure 4, *a* presents the uniaxial compressive strength, *b* presents elastic modulus, *c* presents Poisson's ratio. As shown in Figure 4(a), we can note that the uniaxial compressive strengths of the same lithological rock samples do not differ much, but the differences in uniaxial compressive strengths of different lithological rock samples are more obvious. The uniaxial compressive strength of the rock samples varies from 8.25 to 42.68 MPa, with the average uniaxial compressive strength of 40.8 MPa for the siltstone shales, 25.3 MPa for the shales, 30.3 MPa for the siltstones, 22.3 MPa for the fine sandstones, and 8.85 MPa for the coal rocks. The order of the average uniaxial compressive strength of different lithological rocks is siltstone shales > shales > siltstones> fine

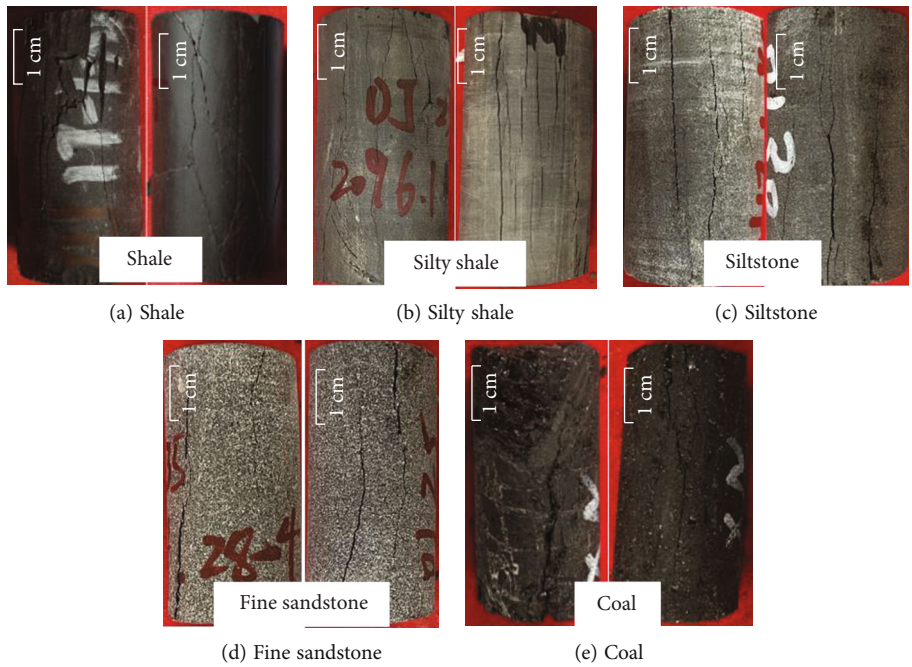

(a) Shale (b) Silty shale (c) Siltstone

(d) Fine sandstone (e) Coal

Figure 3: Failure mode diagram of rock samples under uniaxial compression tests.

sandstones > coal rocks. This may be related to the differences in mineral composition and structure of different lithological rocks. Meanwhile, from Figures 4(b) and 4(c), we can find that the elastic parameters in different lithological rocks differ more obviously, and the elastic modulus of shales is larger and that of coal rocks is smaller, where the elastic modulus of shales is 2-3 times that of sandstones. According to the previous research results, the differences in the elastic modulus of different lithological rocks would affect the fracture penetration ability among different lithological formations, which would affect the longitudinal upward penetration of fractures, thus affecting the extension of longitudinal fractures' height. For different lithological rocks, the sandstones with the characteristics of low elastic modulus and high Poisson's ratios are not conducive to fracturing to form fracture network. The coal rocks with the low elastic modulus and high Poisson's ratios are easy to form fracture network during fracturing transformation due to relatively developed cleats. The shales formation with high elastic modulus and low Poisson's ratios is conducive to fracture network fracturing. This shows that the vertical and horizontal distribution of rocks in different lithological formations of coal measure strata in the study area is complex, resulting in obvious differences in the vertical and horizontal distribution of elastic modulus and Poisson's ratios of rocks, which can lead to different fracturing measures for different lithological reservoirs, and different vertical penetration capacities of fractures, indicating that the differential reconstruction designs should be considered in the fracturing scheme design of different lithological reservoirs. Therefore, when selecting multilayer combined pressure of coal measure formation, interval optimization should be carried out to realize fracture height extension, and appropriate fracturing combination mode should be selected for fracturing transformation.

The above research results show that there are significant differences in the strength parameters and elastic parameters of different lithological rocks of the coal measure strata, combined with the characteristics of rapid spatial and temporal lithological changes, complex lithology, and frequent interstratification of the coal measure strata in the study area, which can cause more obvious differences in the distribution of strength parameters and elastic parameters in the longitudinal and lateral directions of the coal measure strata and more obvious differences among different lithological rocks. This is related to the sedimentary environment and multisource and sedimentary structure of the coal measures strata. This mechanical difference will affect the wellbore instability prevention measures and fracturing measures in different lithologic reservoir sections of coal measure strata.

3.3. Deformation Characteristics. Stress-strain curves of rock samples with different lithologies under uniaxial compression test are shown in Figure 5. It can be seen from Figure 5 that during the loading process, the deformation characteristics of rock samples with different lithology are obviously different. There is a compaction stage in the initial stage of coal rock, while other rock samples are relatively dense and no compaction section is found. The siltstone and fine sandstone have a long elastic deformation phase, whereas the shale and siltstone shale have a short elastic deformation phase, and the siltstone and fine sandstone do not see an obvious plastic deformation section during the loading process. The axial peak strains of siltstone shale, shale, siltstone, fine sandstone, and coal rock in the figure vary more significantly, but the peak strains of different lithological rock samples are less than 1%, which indicates that the different lithological rocks have a certain brittleness. The peak strain of the silty shale is 0.27%, that of the shale is

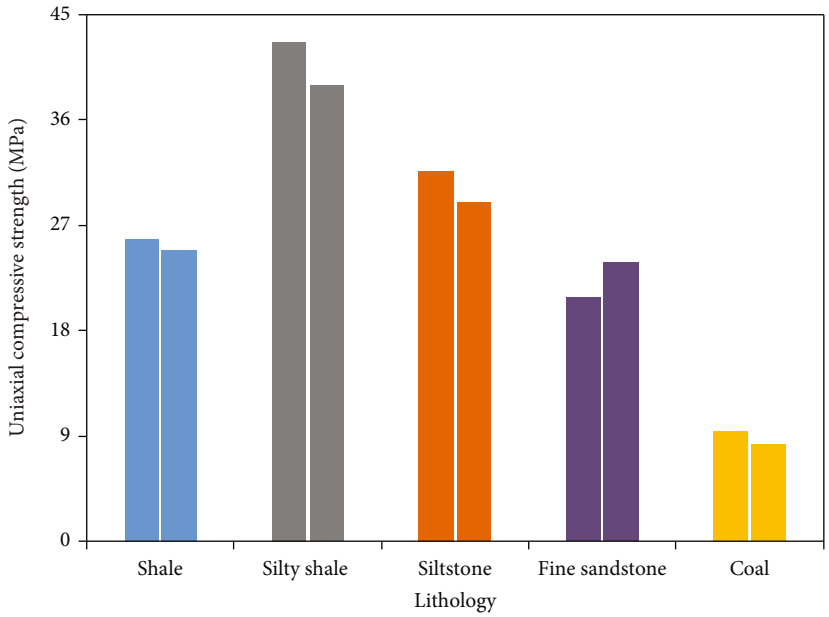

(a) Uniaxial compressive strength

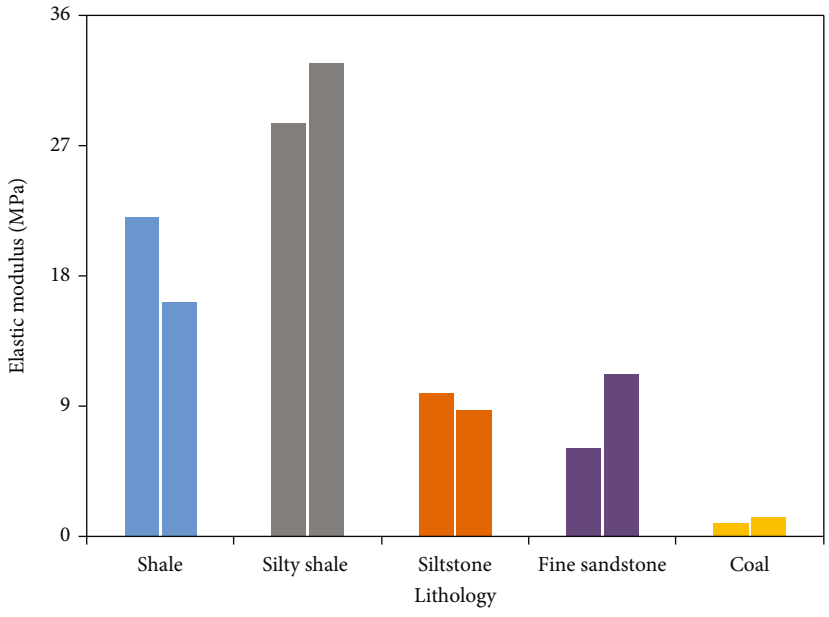

(b) Elastic modulus

Figure 4: Continued.

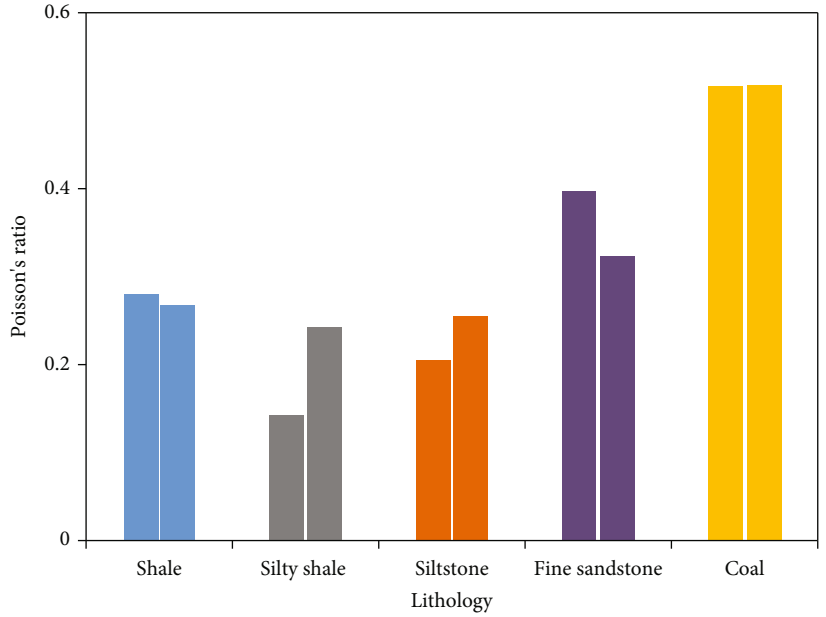

(c) Poisson's ratio

Figure 4: Comparison of uniaxial compression test results of different lithological rock samples.

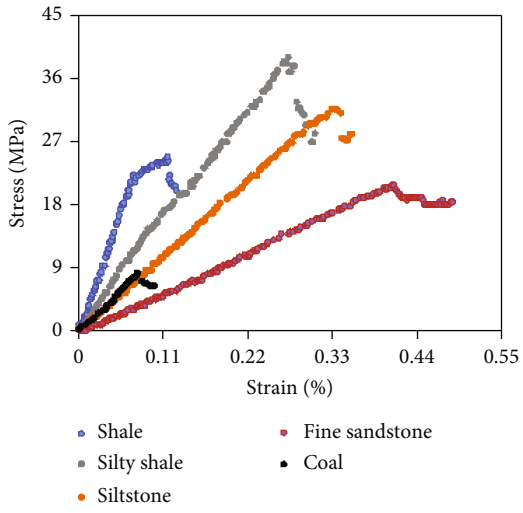

Figure 5: Stress-strain curves of different lithological rock samples under uniaxial compression tests.

0.11%, that of the siltstone is 0.34%, that of the fine sandstone is 0.41%, and that of the coal rock is 0.08%.

4. Discussion

At the same time, according to the stress-strain curve, the total energy, elastic energy, and dissipation energy of the experimental rock sample during continuous loading are further calculated. The total energy U consists of two parts: one part is the elastic strain energy U_e, which is stored in the form of elastic deformation of the rock sample before the peak stress and can be completely released when damage occurs. The other part is the dissipated energy U_d, which is dissipated by the plastic deformation of rock samples and the generation of microcracks before the peak stress, the penetration of the microcracks to form macroscopic cracks when failure occurs so that the energy is dissipated in large quantities, and the relative sliding that occurs between the crack surfaces also consumes energy. All kinds of energy are present simultaneously throughout the process of rock samples from force to damage, only the proportion of which varies in different cases [23]. The total energy expression is [22]:

$$U = U_e + U_d. \tag{4}$$

Under the uniaxial compression test, the total energy and elastic energy absorbed by the rock samples can be expressed, respectively, as [17]:

$$U = \int \sigma_1 d\varepsilon_1 = \sum_{i=0}^{n} \frac{1}{2}(\varepsilon_{1i+1} - \varepsilon_{i1})(\sigma_{1i} + \sigma_{1i+1}), \tag{5}$$

$$U_e = \frac{\sigma_1^2}{2E_0}, \tag{6}$$

where σ_1 and ε_1 are the axial stress (MPa) and axial strain (mm/mm), respectively; σ_{1i} and ε_{1i} are the axial stress (MPa) and axial strain (mm/mm) at point i on the axial stress-strain curve, respectively; E_0 is the initial modulus of elasticity of the rock sample (MPa).

Based on the data of the axial stress, axial strain, radial strain, and confining pressure obtained from compression experiments, the energy evolution curves under various compression tests can be obtained. The energy evolution curves of some rock samples under uniaxial compression tests are shown in Figure 6. The corresponding energy

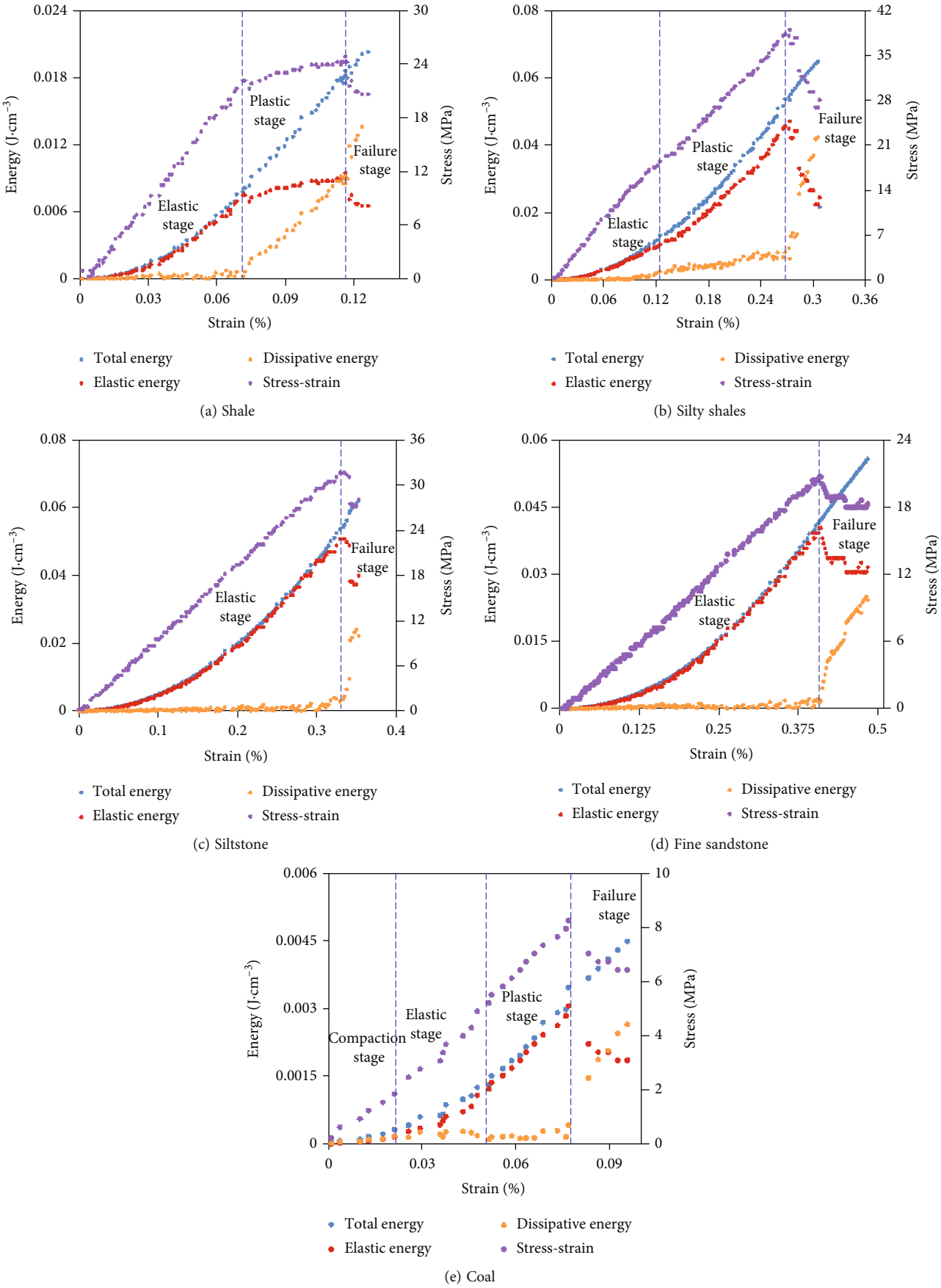

Figure 6: Energy evolution curves of different lithological rock samples under uniaxial compression tests.

Table. 1: Corresponding energy parameters at the peak strain points.

No.	Lithology	U	U_e	U_d	U_e/U
1	Shale	0.02472	0.01501	0.00971	0.61
2		0.01859	0.00944	0.00915	0.51
3	Silty shale	0.03566	0.03194	0.00372	0.90
4		0.05340	0.04710	0.00629	0.88
5	Siltstone	0.05361	0.05075	0.00286	0.95
6		0.05087	0.04780	0.00307	0.94
7	Fine sandstone	0.04183	0.04044	0.00139	0.97
8		0.04129	0.04026	0.00103	0.98
9	Coal	0.00297	0.00253	0.00043	0.85
10		0.00346	0.00305	0.00041	0.88

parameters at the peak point of each rock sample are shown in Table 1. By studying the energy evolution characteristics of rock samples with different lithology, it is found that there are obvious differences in the energy evolution process and energy parameters of rock samples with different lithology. Therefore, the differences in the energy evolution laws of different lithological rock samples are further analyzed.

The energy evolution characteristics of some rock samples with different lithologies are shown in Figure 6. Combined with the stress-strain curves of rock samples, the energy evolution curves of rock samples are divided into different stages:

(1) Compaction stage: Corresponding to the previous stage where the elastic energy is equal to the dissipated energy, in this stage, the deformation of the rock samples increases obviously under the action of low load, and the total energy of the rock samples continues to increase. The dissipated energy curves increase linearly and slowly, and the elastic energy curves increase slowly in a "concave" shape, in which the elastic energy is less than the dissipated energy. The deformation stage of rock samples is the compaction stage. This is because at the initial stage of loading, the original microcracks and micropores of the rock samples are gradually closed, and the dislocation between some internal particles needs to overcome the friction, resulting in more loss in the form of dissipated energy in the total energy, while only a small part of the energy is stored in the form of elastic performance, resulting in less energy absorbed by the rock samples. This is mainly because the cleats of coal rocks are relatively developed, while the rock samples of shale, silty shale, siltstone, and fine sandstone are relatively dense and the cracks are not developed

(2) Elastic stage: With the continuous increase of axial load, the total energy acted on the rock samples also continues to increase, in which the elastic performance and dissipated energy show an increasing trend, and the rising trend of elastic energy is significantly greater than that of dissipated energy. When the elastic performance curve intersects with the dissipated energy curve, the deformation stage of rock samples enters the elastic stage. In this stage, the rock samples change from discontinuous state to approximately continuous state, the elastic energy rises rapidly, and the change trend of the elastic energy curve is the same as that of the total energy curve, which is approximately parallel. The rate of the increase of dissipation energy with increasing strain is very slow or approximately constant, resulting in a significant increase of the differences between the two. At this stage, most of the total energy input from the outside is converted into elastic energy and stored, whereas less energy is dissipated and lost. This stage is mainly the energy storage stage. During the loading process, obvious elastic stages can be seen in different lithological rock samples

(3) Plastic stage: As the axial load continues to increase, the strain gradually increases, resulting in the generation of new cracks and the gradual expansion of existing cracks, and the damage of rock samples increases, which is the dissipated energy gradually increases and the growth rates are accelerated. The dissipated energy curves show a "concave" shape, whereas the elastic performance still increases, but the growth rates slow down, and the elastic energy curves show a "convex" shape. In this stage, the dissipated energy is still small, and the elastic energy still dominates and reaches the maximum at the peak strength. During loading, obvious plastic stages can be seen in the shales, silty shales, and coal rock samples, whereas there is no obvious plastic stage in the siltstone and fine sandstone samples (as shown in Table 1).

(4) Failure stage: This stage is after the corresponding strain at the peak strength. After reaching the peak strength, the microcracks in the rock samples penetrate to form the macrocracks, resulting in the instantaneous release of elastic energy and the sharp rise of dissipated energy, resulting in the destruction and instability of the rock sample

Under uniaxial compression tests, the variation laws of the total energy before peak strain of different lithological rock samples are shown in Figure 7(a). The variation trends of total energy of different lithological rock samples in the figure before peak strain are the same, in which the total energy increases with the increase of the strain, reflecting that the rock samples continue to increase under the action of the external forces. There are differences in the total energy corresponding to different lithological rock samples under the same strain condition. For example, when the strain is about 0.1%, the total energy of different lithological rock samples is shale 0.0149 J/cm^3, silty shale 0.0081 J/cm^3, siltstone 0.0051 J/cm^3, and fine sandstone 0.0022 J/cm^3. This shows that before the failure of different lithological rock samples, at the initial stage of loading, the strain of shale is

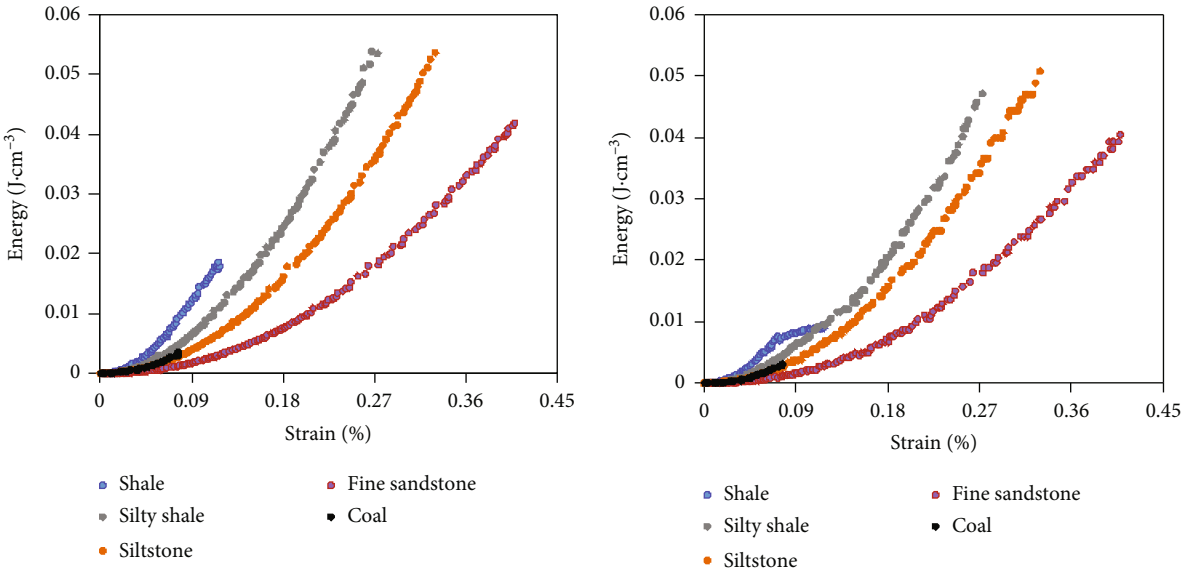

(a) Total energy before peak

(b) Elastic properties before peak

Figure 7: The energy parameters before peak strain of different lithological rocks under uniaxial compression tests.

the largest, while that of fine sandstone is the smallest (it should be noted that coal rocks have been damaged under low load). It can also be observed in the figure that there are obvious differences in the total energy of different lithological rock samples at the peak strain.

Under the uniaxial compression tests, the variation laws of the elastic properties before peak strain of different lithological rock samples are shown in Figure 7(b). From Figure 7(b), we can note that the variation trends of elastic energy before peak strain of different lithological rock samples are the same with Figure 7(a), indicating that the energy absorbed by the rock samples continue to increase under the continuous action of external forces. At the same time, the corresponding elastic energy of rock samples with different lithology at peak strain is very different, as shown in Table 1, which reflects the difference of absorbed energy when rock samples are damaged. Among them, the maximum average elastic energy of siltstone at the peak strength is 0.05224 J/cm^3, fine sandstone is 0.04035 J/cm^3, silty shale is 0.03952 J/cm^3, shale is 0.0122 J/cm^3, and coal rock is 0.00279 J/cm ^{3}. This shows that when the different lithological rock samples are damaged, the energy stored in siltstone is the largest, the energy released in the event of damage will be the largest, and the coal rock is the smallest. According to Figure 7, they are reflected that the energy before peak strain is different among different lithological rocks in coal measure strata, indicating that there are differences in energy evolution laws among different lithological rock, reflecting that there is obvious heterogeneity among different lithological rocks, and there are differences in the energy consumed during destruction of different lithological rocks, which may result in different energy consumption for hydraulic fracturing of different lithological formations. This also means that customized fracturing design should be considered in the fracturing design of different lithological formations in the coal measure strata in the eastern margin of Ordos Basin.

5. Conclusions

In this paper, the mechanical behaviors of the rocks of the coal measure strata from the Shanxi Formation in the eastern margin of Ordos Basin are investigated, the compressive characteristics, deformation characteristics, and failure modes of different lithological rocks are studied, and the energy evolution laws of different lithological rocks are also discussed. The following conclusions were obtained:

(1) There are obvious differences in the mechanical properties of different lithological rocks in the coal measure strata, the compressive strength of the silty shales is the largest with an average value of 40 MPa, and the compressive strength of the coals is the smallest with an average value of 8.85 MPa, resulting in the strong heterogeneity, which can cause different wellbore instability prevention measures and fracturing reconstruction measures in different lithological reservoirs

(2) Under the uniaxial compression tests, the peak strain of different lithological rocks is obviously different, and the denaturation characteristics are obviously different. The rock failure modes are mainly the tensile fracture mode, indicating that rock samples have strong brittle characteristics

(3) With the increase of the strain, the total energy of different lithological rocks increases, and the elastic energy first increases and then decreases rapidly, whereas the dissipated energy first increases slowly and then increases rapidly. The energy at the peak strain is different, suggesting that there are obvious differences in the energy evolution laws of different lithological rocks

Data Availability

The data used to support the findings of this study are included within the article.

Conflicts of Interest

The authors declare that there is no conflict of interests regarding the publication of this paper.

Authors' Contributions

Xiong Jian contributed to the experiment, data analysis, writing-reviewing; Wu Jianjun contributed to the experiment, writing-reviewing; Liu Junjie contributed to the data analysis, writing-reviewing; Li Bing contributed to the data analysis; Liu Xiangjun contributed to the data analysis; Lixi Liang contributed to the investigation, data analysis.

Acknowledgments

This research is supported by the Science and Technology Cooperation Project of the CNPC-SWPU Innovation Alliance (Grant No. 2020CX030000), and the Young Scientific and Technological Innovation Team of Rock Physics in Unconventional Strata of Southwest Petroleum University (No. 2018CXTD13).

References

[1] C. Zou, S. Pan, and Q. Hao, "On the connotation, challenge and significance of China's "energy independence" strategy," *Petroleum Exploration and Development*, vol. 47, no. 2, pp. 449–462, 2020.

[2] Y. Li, D. Tang, P. Wu et al., "Continuous unconventional natural gas accumulations of Carboniferous-Permian coal-bearing strata in the Linxing area, northeastern Ordos basin, China," *Journal of Natural Gas Science & Engineering*, vol. 36, pp. 314–327, 2016.

[3] Y. Li, J. Yang, Z. Pan, S. Meng, K. Wang, and X. Niu, "Unconventional natural gas accumulations in stacked deposits: a discussion of Upper Paleozoic coal-bearing strata in the east margin of the Ordos Basin, China," *Acta Geologica Sinica*, vol. 93, no. 1, pp. 111–129, 2019.

[4] M. Shangzhi, H. Bing, Z. Jian, T. Peng, and X. Zhenyu, "Experimental research on hydraulic fracture propagation through mixed layers of shale, tight sand and coal seam," *Journal of China Coal Society*, vol. 41, no. 1, pp. 221–227, 2016.

[5] S. Z. Meng, Y. Li, J. Z. Wang, G. Gu, Z. Wang, and X. Xu, "Coproduction feasibility of "Three gases" in coal measures: Discussion based on field test well," *Journal of China Coal Society*, vol. 43, no. 1, pp. 168–174, 2018.

[6] J. Shen, Y. Qin, B. Zhang, G. Z. Li, and Y. L. Shen, "Superimposing gas-bearing system in coal measures and its compatibility in Linxing Block, East Ordos Basin," *Journal of China Coal Society*, vol. 43, no. 6, pp. 1614–1619, 2018.

[7] Y. Li, M. Long, L. Zuo, W. Li, and W. Zhao, "Brittleness evaluation of coal based on statistical damage and energy evolution theory," *Journal of Petroleum Science and Engineering*, vol. 172, pp. 753–763, 2019.

[8] Y. Li, D. Jia, M. Wang et al., "Hydraulic fracturing model featuring initiation beyond the wellbore wall for directional well in coal bed," *Journal of Geophysics and Engineering*, vol. 13, no. 4, pp. 536–548, 2016.

[9] L. I. Yuwei, L. O. Min, T. A. Jizhou, C. H. Mian, and F. U. Xiaofei, "A hydraulic fracture height mathematical model considering the influence of plastic region at fracture tip," *Petroleum Exploration and Development*, vol. 47, no. 1, pp. 184–195, 2020.

[10] Y. Zou, S. Li, X. Ma, S. Zhang, N. Li, and M. Chen, "Effects of CO2-brine-rock interaction on porosity/permeability and mechanical properties during supercritical-CO2 fracturing in shale reservoirs," *Journal of Natural Gas Science and Engineering*, vol. 49, pp. 157–168, 2018.

[11] Y. Li, H. Li, G. Chen, K. Geng, L. Cao, and T. Liang, "On the compressional extensional tectonic environment for the formation of Jiaodong gold deposit, Shandong Province," *Geotectonics and Metallogeny*, vol. 4, no. 6, pp. 1117–1132, 2019.

[12] Y. Li, J. Yang, Z. Pan, and W. Tong, "Nanoscale pore structure and mechanical property analysis of coal: An insight combining AFM and SEM images," *Fuel*, vol. 260, article 116352, 2020.

[13] Y. Li, J.-Q. Chen, J.-H. Yang, J.-S. Liu, and W.-S. Tong, "Determination of shale macroscale modulus based on microscale measurement: a case study concerning multiscale mechanical characteristics," *Petroleum Science*, vol. 19, no. 3, pp. 1262–1275, 2022.

[14] H. Wang, M. He, F. Pang, Y. Chen, and Z. Zhang, "Energy dissipation-based method for brittleness evolution and yield strength determination of rock," *Journal of Petroleum Science & Engineering*, vol. 200, 2021.

[15] Y. Li, D. Jia, Z. Rui, J. Peng, C. Fu, and J. Zhang, "Evaluation method of rock brittleness based on statistical constitutive relations for rock damage," *Journal of Petroleum Science and Engineering*, vol. 153, pp. 123–132, 2017.

[16] E. Stavropoulou, C. Dano, and M. Boulon, "Shear response of wet weak carbonate rock/grout interfaces under cyclic loading," *Rock Mechanics and Rock Engineering*, vol. 54, no. 6, pp. 2791–2813, 2021.

[17] P. Rai, "A comparative investigation of inter-row delay timing vis-à-vis some rock properties on high sandstone benches," *Indian Journal of Engineering and Materials Sciences (IJEMS)*, vol. 27, no. 1, pp. 112–119, 2020.

[18] C. Li, M. Ostadhassan, A. Abarghani, A. Fogden, and L. Kong, "Multi-scale evaluation of mechanical properties of the Bakken shale," *Journal of Materials Science*, vol. 54, no. 3, pp. 2133–2151, 2019.

[19] P. Bagde and V. Petroš, "Fatigue properties of intact sandstone samples subjected to dynamic uniaxial cyclical loading," *International Journal of Rock Mechanics and Mining Sciences*, vol. 42, no. 2, pp. 237–250, 2005.

[20] S. Akdag, M. Karakus, G. D. Nguyen, A. Taheri, and T. Bruning, "Evaluation of the propensity of strain burst in brittle granite based on post-peak energy analysis," *Underground Space*, vol. 6, no. 1, pp. 1–11, 2021.

[21] Z. Chen, C. He, W. Dong, G. Ma, and C. Pei, "Physico-mechanical properties and its energy damage evolution mechanism of the jurassic and cretaceous argillaceous sandstone in northern Xinjiang," *Rock and Soil Mechanics*, vol. 39, no. 8, pp. 2873–2885, 2018.

[22] J. Jiang, S. Chen, J. Xu, and Q. Liu, "Mechanical properties and energy characteristics of mudstone under different containing moisture states," *Journal of China Coal Society*, vol. 43, no. 8, pp. 2217–2224, 2018.

[23] X. Yang, H. Cheng, and Y. Pei, "Study on rock deformation and post peak energy evolution under different loading modes," *Journal of Rock Mechanics and Engineering*, vol. 39, no. A2, pp. 3229–3236, 2020.

[24] C. Hongde, L. Jie, Z. Chenggong, C. Lixue, and C. Lijun, "Discussion of sedimentary environment and its geological enlightenment of Shanxi Formation in Ordos Basin," *Acta Petrologica Sinica*, vol. 27, no. 8, pp. 2213–2229, 2011.

[25] L. Kuang, D. O. Dazhong, H. E. Wenyuan et al., "Geological characteristics and development potential of transitional shale gas in the east margin of the Ordos Basin, NW China," *Petroleum Exploration and Development*, vol. 47, no. 3, pp. 471–482, 2020.

[26] W. U. Jin, W. A. Hongyan, S. H. Zhensheng et al., "Favorable lithofacies types and genesis of marine-continental transitional black shale: a case study of Permian Shanxi Formation in the eastern margin of Ordos Basin, NW China," *Petroleum Exploration and Development*, vol. 48, no. 6, pp. 1315–1328, 2021.

[27] Y. Chen, D. Ma, Y. Xia, C. Guo, F. Yang, and K. Shao, "Characteristics of the mud shale reservoirs in coal-bearing strata and resources evaluation in the eastern margin of the Ordos Basin, China," *Energy Exploration & Exploitation*, vol. 38, no. 2, pp. 372–405, 2020.

[28] Y. Qi, Y. Ju, J. Cai et al., "The effects of solvent extraction on nanoporosity of marine-continental coal and mudstone," *Fuel*, vol. 235, pp. 72–84, 2019.

[29] T. Ma, C. Yang, P. Chen, X. Wang, and Y. Guo, "On the damage constitutive model for hydrated shale using CT scanning technology," *Journal of Natural Gas Science and Engineering*, vol. 28, pp. 204–214, 2016.